Journal of Thermal Analysis and Calorimetry, Vol. 91 (2008) 1, 267–274

A THERMOGRAVIMETRIC AND INFRARED EMISSION SPECTROSCOPIC STUDY OF ALUNITE

R. L. Frost and Daria Wain*

Inorganic Materials Research Program, School of Physical and Chemical Sciences, Queensland University of Technology, GPO Box 2434, Brisbane Queensland 4001, Australia

Thermogravimetric and differential thermogravimetric analysis has been used to characterize alunite of formula $[K_2(Al^{3+})_6(SO_4)_4(OH)_{12}]$. Thermal decomposition occurs in a series of steps (a) dehydration up to 225°C, (b) well defined dehydroxylation at 520°C and desulphation which takes place as a series of steps at 649, 685 and 744°C.

The alunite minerals were further characterized by infrared emission spectroscopy (IES). Well defined hydroxyl stretching bands at around 3463 and 3449 cm^{-1} are observed. At 550°C all intensity in these bands is lost in harmony with the thermal analysis results. OH stretching bands give calculated hydrogen bond distances of 2.90 and 2.84–7 Å. These hydrogen bond distances increase with increasing temperature. Characteristic $(SO_4)^{2-}$ stretching modes are observed at 1029.5, 1086 and 1170 cm^{-1}. These bands shift to lower wavenumbers on thermal treatment. The intensity in these bands is lost by 550°C.

Keywords: *alunite, ammonioalunite, jarosite, natroalunite, Raman spectroscopy, sulphate*

Introduction

Interest in the chemistry of alunites stems from a number of reasons. Firstly, because of the possible discovery of alunites on Mars [1, 2]. Such a find implies the presence of water on Mars either at present or at some time in the planetary past [3, 4]. Interest in such minerals and their thermal stability rests with the possible identification of these minerals and related dehydrated paragenetically related mineral on planets and on Mars. There have been many studies on related minerals such as the Fe(II) and Fe(III) sulphate minerals [5–10]. Secondly, alunites are found in soils and evaporate deposits. The importance of alunite formation and its decomposition depends upon its presence in soils, sediments and evaporate deposits [11]. These types of deposits have formed in acid soils where the pH is less than 3.0 pH units [12]. Such acidification results from the oxidation of pyrite which may be from bacterial action or through air-oxidation. Thirdly, alunites are important from an environmental point of view. Alunites are minerals which can function as collectors of heavy metals and low concentrations can be found in the natural alunites. Such minerals can act as a significant environmental sink [13]. One of the difficulties associated with the analysis of alunites is that they are often poorly crystalline, making detection using XRD techniques difficult. Another problem associated with the study of alunites is their thermodynamic stability [14]. Often the minerals are formed from acid-sulfate rich environments such as acid mine drainage and acid-sulfate soils and as such their solubility is controlled by the climatic conditions in particular the temperature.

Alunites are a group of minerals which form part of the alunite supergroup [15]. The general formula is given by $DG_3(TO_4)_2(OH,H_2O)_6$ where the *D* sites are occupied by monovalent cations such as K, Na, NH_4, H_3O^+ and others, divalent cations such as Ca, Ba, Sr, Pb, trivalent cations for example Bi; and *G* is the trivalent cation either Al of Fe^{3+}; and *T* is S^{6+}, As^{5+} or P^{5+}. Alunites can be divided into alunites and jarosites simply depending on whether the concentration of Al is >Fe (alunites) or Fe>Al (jarosites) [14]. Of course solid solution formation can exist across a wide range of concentrations and substitutions. Common members of the alunite group are alunite $KAl_3(SO_4)_2(OH)_6$, natroalunite $NaAl_3(SO_4)_2(OH)_6$, ammonioalunite $NH_4Al_3(SO_4)_2(OH)_6$, sclossmacherite $(H_3O^+,Ca^{2+})Al_3(SO_4)_2(OH)_6$. The structure of alunites is well known [16–18]. The structure of alunites is trigonal with a 6.990, c 16.905 Å space group R3m, with *Z*=3.

There have been a significant number of vibrational spectroscopic studies of alunites [19–26]. The number of Raman studies have been few [27–29]. According to Ross the infrared spectrum of alunite consists of the ν_1 mode at 1030 cm^{-1}, the ν_2 mode at 475 cm^{-1}, the ν_3 mode at 1170, 1086 cm^{-1} and the ν_4 mode at 632 and 605 cm^{-1} [30]. The observation of multiple bands for the ν_3 and ν_2 modes implies the

* Author for correspondence: r.frost@qut.edu.au

1388–6150/$20.00
© 2008 Akadémiai Kiadó, Budapest
Akadémiai Kiadó, Budapest, Hungary
Springer, Dordrecht, The Netherlands

symmetry of the sulphate is reduced from $Td \Rightarrow C_{3v}$. Indeed vibrational spectroscopy has been used to refine the space group of alunites [31]. Isomorphism in alunites has been studied by infrared spectroscopy [21]. Vibrational spectroscopy allows a better method for the study of these minerals. Infrared spectroscopy has been used to study jarosite minerals but failed to detect cationic differences in the jarosite structures [27, 32–36]. Raman spectroscopy has been used to study jarosites but some previous studies failed to study the complete spectra [27, 33, 37]. Further the lack of crystallinity of the synthetic samples studied may have made the collection of Raman spectral data difficult. Most studies have involved the use of synthetic jarosites [38].

Thermal analysis has proven extremely useful for determining the stability of minerals [39–47]. In this work, as part of our studies of secondary mineral formation, we report the infrared emission and thermal analysis of selected alunites.

Experimental

Minerals

The alunites were obtained from the Mineralogical Research Company. The minerals were phase analysed by powder X-ray diffraction and were analysed by chemical composition by EDX methodology.

Methods

X-ray diffraction

X-ray diffraction (XRD) patterns were recorded using CuK_α radiation (n=1.5418 Å) on a Philips PANalytical X'Pert PRO diffractometer operating at 40 kV and 40 mA with 0.125° divergence slit, 0.25° anti-scatter slit, between 3 and 15° (2θ) at a step size of 0.0167°. For low angle XRD, patterns were recorded between 1 and 5° (2θ) at a step size of 0.0167° with variable divergence slit and 0.5° anti-scatter slit.

Thermal analysis

Thermal decomposition of the alunite minerals was carried out in a TA® Instruments incorporated high-resolution thermogravimetric analyzer (series Q500) in a flowing nitrogen atmosphere (60 cm^3 min^{-1}). Approximately 35 mg of each sample underwent thermal analysis, with a heating rate of 5°C min^{-1}, with resolution of 6 from 25 to 1000°C. With the isothermal, isobaric heating program of the instrument the furnace temperature was regulated precisely to provide a uniform rate of decomposition in the main decomposition stage.

Infrared spectroscopy

Infrared spectra were obtained using a Nicolet Nexus 870 FTIR spectrometer with a smart endurance single bounce diamond ATR cell. Spectra over the 4000–525 cm^{-1} range were obtained by the co-addition of 64 scans with a resolution of 4 cm^{-1} and a mirror velocity of 0.6329 cm s^{-1}. Spectral manipulation such as baseline adjustment, smoothing and normalization was performed using the GRAMS® software package (Galactic Industries Corporation, Salem, NH, USA).

FTIR emission spectroscopy was carried out on a Nicolet Nexus 870 FTIR spectrometer equipped with a TGS detector, which was modified by replacing the IR source with an emission cell. A description of the cell and principles of the emission experiment have been published elsewhere [48–51]. Approximately 0.2 mg of alunite was spread as a thin layer (approximately 0.2 microns) on a 6 mm diameter platinum surface and held in an inert atmosphere within a nitrogen-purged cell during heating. The infrared emission cell consists of a modified atomic absorption graphite rod furnace, which is driven by a thyristor-controlled AC power supply capable of delivering up to 150 amps at 12 volts. A platinum disk acts as a hot plate to heat the smectite sample and is placed on the graphite rod. An insulated 125-μm type R thermocouple was embedded inside the platinum plate in such a way that the thermocouple junction was <0.2 mm below the surface of the platinum. Temperature control of ±2°C at the operating temperature of the smectite sample was achieved by using a Eurotherm Model 808 proportional temperature controller, coupled to the thermocouple. The design of the IES facility is based on an off axis paraboloidal mirror with a focal length of 25 mm mounted above the heater capturing the infrared radiation and directing the radiation into the spectrometer. The assembly of the heating block, and platinum hot plate is located such that the surface of the platinum is slightly above the focal point of the off axis paraboloidal mirror. By this means the geometry is such that approximately 3 mm diameter area is sampled by the spectrometer. The spectrometer was modified by the removal of the source assembly and mounting a gold-coated mirror, which was drilled through the centre to allow the passage of the laser beam. The mirror was mounted at 45°, which enables the IR radiation to be directed into the FTIR spectrometer.

In the normal course of events, three sets of spectra are obtained: firstly the black body radiation over the temperature range selected at the various temperatures, secondly the platinum plate radiation is obtained at the same temperatures and thirdly the spectra from the platinum plate covered with the sample. Normally only one set of black body and platinum radiation is required. The

emittance spectrum at a particular temperature was calculated by subtraction of the single beam spectrum of the platinum backplate from that of the platinum+sample, and the result rationed to the single beam spectrum of an approximate blackbody (graphite). This spectral manipulation is carried out after all the spectral data has been collected. The emission spectra were collected at intervals of 50°C over the range 200–750°C. The time between scans (while the temperature was raised to the next hold point) was approximately 100 s. It was considered that this was sufficient time for the heating block and the powdered sample to reach temperature equilibrium. The spectra were acquired by coaddition of 64 scans for the whole temperature range (approximate scanning time 45 s), with a nominal resolution of 4 cm^{-1}. Good quality spectra can be obtained providing the sample thickness is not too large. If too large a sample is used then the spectra become difficult to interpret because of the presence of combination and overtone bands.

Spectral manipulation such as baseline adjustment, smoothing and normalisation was performed using the Spectracalc software package (Galactic Industries Corporation, Salem, NH, USA).

Results and discussion

Thermogravimetric analysis of potassium alunite

The thermogravimetric analysis of the alunite from Italy is shown in Fig. 1. The mass spectra of evolved gases are reported in Figs 2a and 2b. Three major processes occur for the thermal decomposition of alunite. These are dehydration, dehydroxylation and desulphation. The details of these processes are listed below.

Mechanism for decomposition of potassium alunite

Step 1 dehydration – temperature up to ~220°C

$$KAl_3(SO_4)_2(OH)_6 \cdot xH_2O \rightarrow KAl_3(SO_4)_2(OH)_6 + xH_2O$$

This step represents the dehydration step and occurs over a long temperature range starting at ~50°C and continues up to 225°C. The wide temperature range for dehydration shows that water is strongly adsorbed to the alunite surfaces. There is a mass loss of 1.3% for this step.

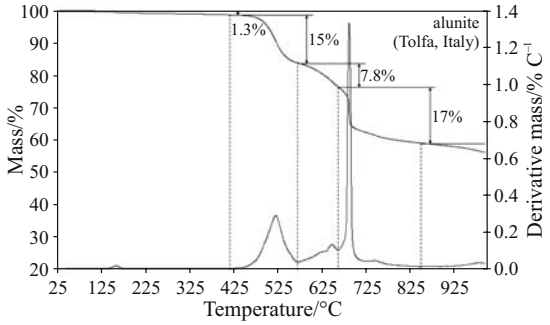

Fig. 1 Thermogravimetric and differential thermogravimetric analysis of alunite from Italy

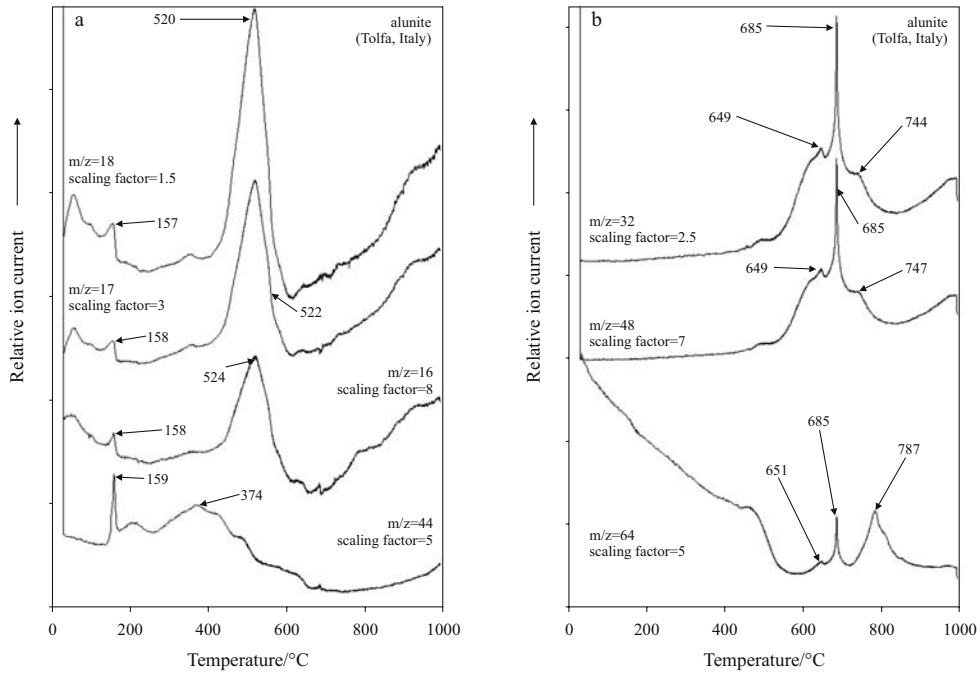

Fig. 2 Ion current curves of evolved water vapour a – *m*/*z*=16,17,18,44 and b – *m*/*z*=32,48,64

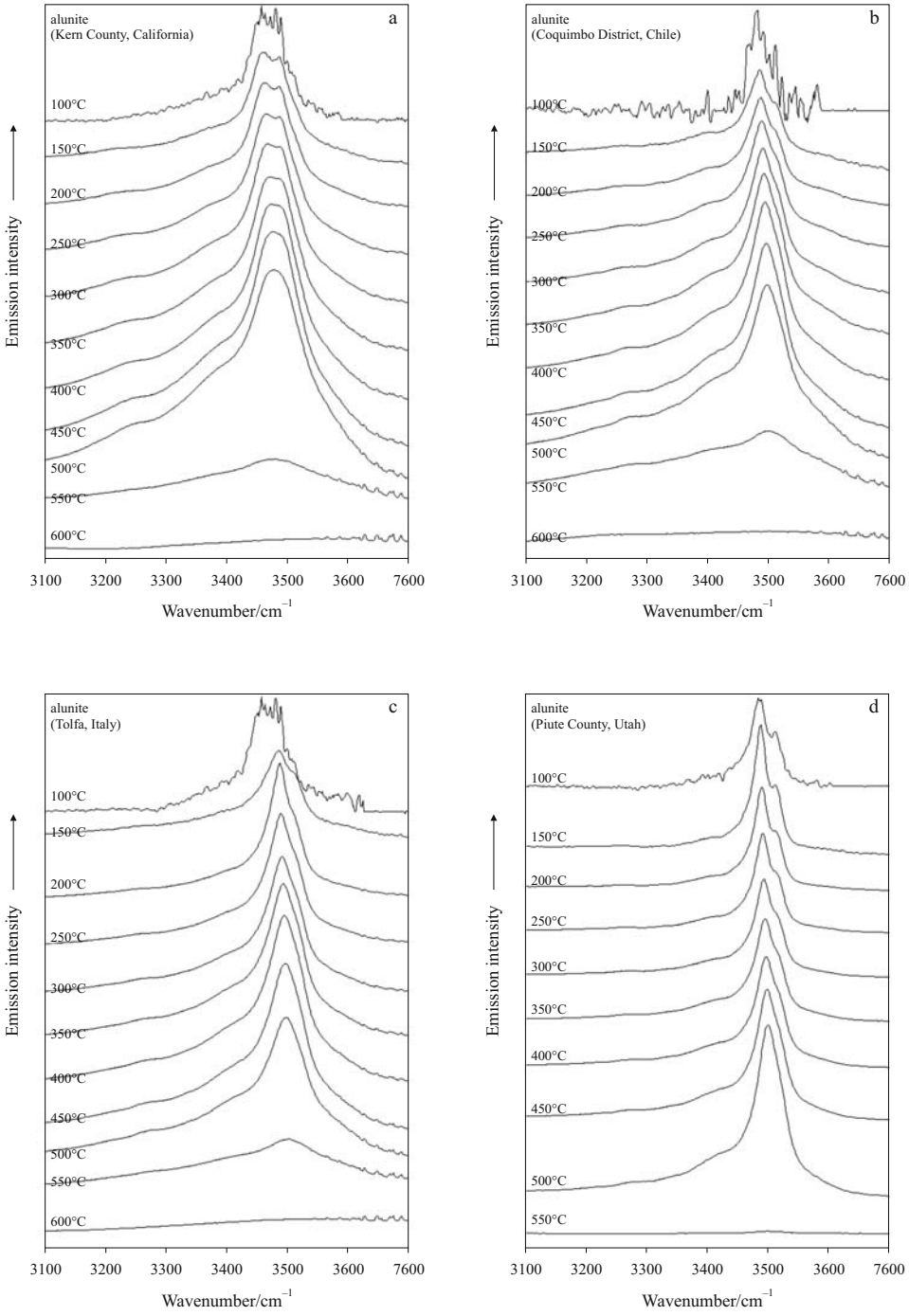

Fig. 3 Infrared spectra of the hydroxyl stretching region from 100 to 600°C of alunites from a – California, b – Chile, c – Italy, d – Utah

Step 2 dehydroxylation – at 520°C

$$KAl_3(SO_4)_2(OH)_6 \rightarrow KO_{1/2}Al_3(SO_4)_2 + 3H_2O$$

This step represents the loss of the hydroxyl units from the alunite structure. Figure 1 shows two mass loss steps at 520 and 685°C with mass losses of 15.0 and 7.8% for a total of 22.8%. The *MW* of alunite is 414 g mol^{-1} and the theoretical mass% of OH units is 24.6%. Thus there is ~4.0% mass loss per OH unit.

The ion current curves for the evolved gases show for m/z=18 and m/z=16 a mass gain at around 158°C (Fig. 4a). A further mass gain of water vapour occurs at 520°C. At these two temperatures OH units are lost from the alunite structure. The mass gain in the MS curves corresponds precisely with the mass loss in the TG curves.

Step 3 desulphation – loss of sulphate – temperature 649, 685 and around 744°C

$$KO_3Al_3(SO_4)_2 \rightarrow 1/2K_2SO_4+SO_3+1.5Al_2O_3+2.5O_2$$

$$K_2SO_4 \rightarrow SO_3+K_2O$$

and

$$K_2O+Al_2O_3 \rightarrow 2KAlO_2$$

The TG and DTG curves show a large mass loss of 17.0% at 680°C. The ion current curves for *m*/*z*=64, 48 and 32 all show peaks at 649, 685 and 744°C confirming the loss of sulphate at these temperatures.

Infrared emission spectroscopy of the OH stretching region

The IES spectra of the OH stretching region of alunites from (a) California, (b) Chile, (c) Italy and (d) Utah are shown in Figs 3–d. A comparison of the room temperature band component analysed infrared spectra are displayed in Fig. 4. Alunite infrared spectra in the OH stretching region show bands at 3463, 3449 and 3396 cm^{-1} for the California alunite; 3510, 3483 and 3428 cm^{-1} for the Utah alunite; 3510, 3471, 3432 cm^{-1} for the alunite from Italy and 3510, 3469 and 3422 cm^{-1} for the alunite from Chile (Fig. 2). Serna *et al*. states that the alunite cell is rhombohedral and that under the space group D_{3d}^5, there should be only two OH stretching vibrations [27]. Serna *et al.* reported Raman bands at 3508 and 3481 cm^{-1} for (K-al) 3488, 3452 cm^{-1} (Na-al), 3492 cm^{-1} (H_3O^+-al) [27]. Studies have shown a strong correlation between OH stretching frequencies and both O···O bond distances and H···O hydrogen bond distances [52–55]. Libowitzky (1999) showed that a regression function can be employed relating the hydroxyl stretching frequencies with regression coefficients better than 0.96 using infrared spectroscopy [56]. The function is described as: $\nu_1 = (3592–304)\cdot 109^{\frac{-d(O-O)}{0.1321}}$ cm^{-1}. Thus OH---O hydrogen bond distances may be calculated using the Libowitzky empirical function. The values of the OH stretching bands lead to an estimation of hydrogen bond distances. For alunite the bands at 3510 and 3483 cm^{-1} lead to hydrogen bond distances of 2.909 and 2.872 Å. Slight differences in hydrogen bond distances are observed for the other alunites. These hydrogen bond distances appear to fall into two groups at around 2.90 and 2.84–2.87 Å. X-ray crystallographic studies give a hydrogen bond distance of 2.92 Å which is in excellent agreement with the values estimated from the Raman OH stretching wavenumbers. It is suggested that two hydrogen bonds of slightly different strengths exist for alunites.

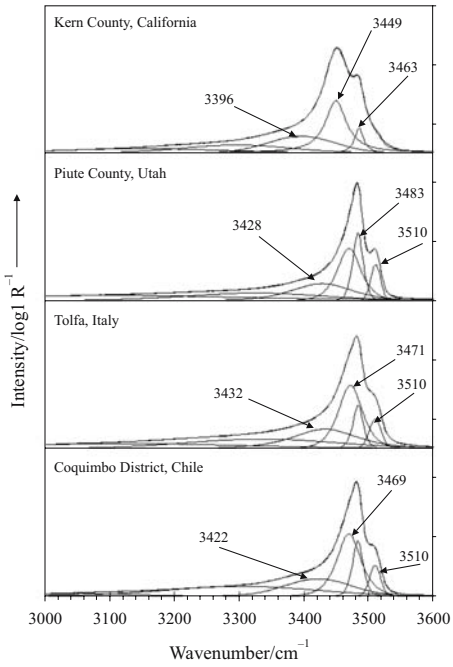

Fig. 4 Band component analysis of the infrared spectra of the hydroxyl stretching region of alunites from a – California, b – Chile, c – Italy, d – Utah at ambient temperature

Infrared emission spectroscopy of the 650 to 1450 cm^{-1} region

Alunites contain sulphate and hydroxyl units which lend themselves to study by vibrational spectroscopy. Sulphates are readily detected by the range of techniques offered by infrared spectroscopy. In aqueous systems, the sulphate anion is of T_d symmetry and is characterised by Raman bands at 981 cm^{-1} (ν_1), 451 cm^{-1} (ν_2), 1104 cm^{-1} (ν_3) and 613 cm^{-1} (ν_4). Reduction in symmetry in the crystal structure of sulphates such as alunites will cause the splitting of these vibrational modes. In 1937 Hendriks proposed the space group R3m for alunite [57]. Later studies based upon refinement of the X-ray crystallography of both synthetic and natural alunites gave the space group as R3barm with a D_{3d}^5 space group [58, 59]. Thus six sulphate fundamentals should be observed. Ross in Farmer (Chapter 18) reports the results of the infrared spectra of alunite [30]. Multiple ν_3 (1170 and 1086 cm^{-1}) and ν_4 (632 and 605 cm^{-1}) bands are observed showing the loss of symmetry in the alunite structure. The symmetric stretching ν_1 mode of the sulphate units was found at 1030 cm^{-1} and the ν_2 mode at 475 cm^{-1}. Ross lists three bending modes at 802, 780 and 605 cm^{-1}. Other studies of the infrared spectra of alunites have been undertaken [60, 61]. Many studies compared the spectra of alunites with that of jarosites and it was suggested that there was no cationic influence [61]. However such a conclusion is

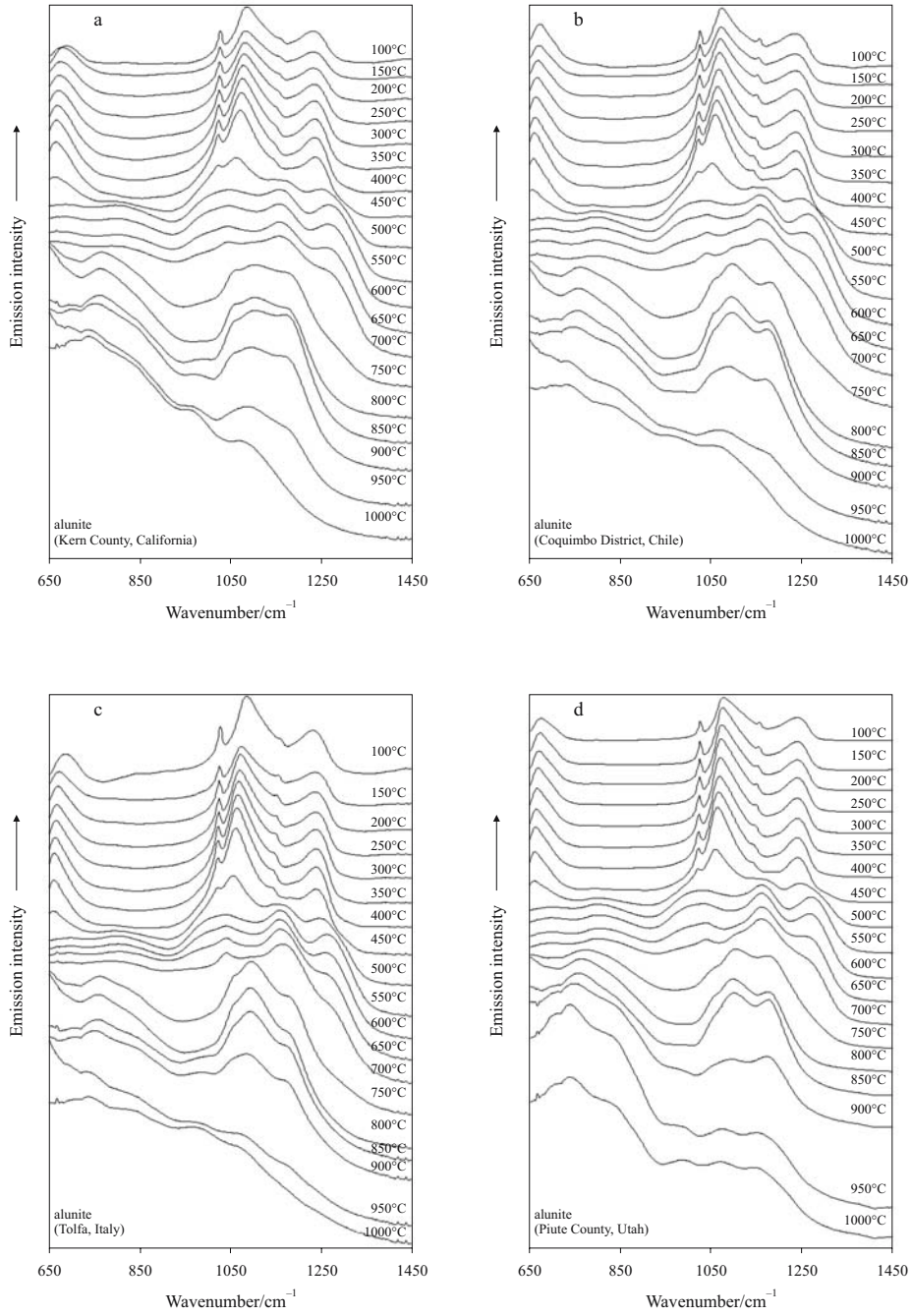

Fig. 5 Infrared spectra of the 650 to 1450 cm^{-1} region over the temperature range 100 to 600°C of alunites from a – California, b – Chile, c – Italy, d – Utah

questionable. Other workers basically gave a catalogue of infrared spectra many of which were incomplete [60].

The infrared emission spectra in the 650 to 1450 cm^{-1} region of alunites from (a) California, (b) Chile, (c) Italy, (d) Utah are shown in Figs 5a–d. The band at 1029.5 cm^{-1} is assigned to the $(SO_4)^{2-}$ symmetric stretching mode. Farmer reports the band at 1030 cm^{-1} for K-alunite . The band shows a shift to lower wavenumbers upon thermal treatment. The band is observed at 1028.9 cm^{-1} at 200°C and at 1027.8 cm^{-1} at 400°C. The intensity of the band approaches zero by 500°C. Two bands are observed at 1095 and 1165 cm^{-1} and are assigned to the $(SO_4)^{2-}$ antisymmetric stretching modes. Infrared bands for alunite for these vibrations were reported by Farmer to be at 1086 and 1170 cm^{-1}. The broad band at 1240 cm^{-1} is ascribed to OH deformation modes. It is noted the intensity of these bands decreases with increased temperature rise until 500°C where the spectral profile changes significantly. The band at 686 cm^{-1} is assigned to the $(SO_4)^{2-}$ bending mode. The intensity in this band is lost by 550°C. Farmer re-

ported a band at 632 cm^{-1} and attributed this band to the ν_4 bending mode [30]. A band at 685 cm^{-1} was tabled for the ν_4 bending mode of $(SO_4)^{2-}$ for jarosite. So it appears that this value for alunite is in error or a misprint. Over the temperature range 550 to 700°C, the spectral profile of the thermally treated alunites is a broad almost featureless spectrum; yet after 700°C a spectrum of the thermally decomposed alunite shows greater intensity. These peaks are attributed to the final decomposition product of the alunite. The IE spectra of the four alunites are identical over the temperature range studied.

Conclusions

Alunites show characteristic thermogravimetric patterns with thermal decomposition steps (a) dehydration up to 225°C (b) well defined dehydroxylation at 520°C and desulphation which takes place as a series of steps at 649, 685 and 744°C.

The alunite mineral group can be characterised by their infrared emission spectra. Intensity loss in the OH stretching modes by 550°C is in harmony with the thermogravimetric results which show dehydroxylation at 520°C.

It is very important to be able to thermally characterise minerals such as alunite which may be found on planets such as Mars. The existence of alunites on Mars would confirm the presence of water at some time in the past as such minerals are only formed from solution. The thermal stability of alunites is most important as there is a need to find the temperature range over which the minerals are stable, since wide temperature ranges are likely on planets.

Acknowledgements

The financial and infra-structure support of the Queensland University of Technology Inorganic Materials Research Program of the School of Physical and Chemical Sciences is gratefully acknowledged. The Australian Research Council (ARC) is thanked for funding.

References

1 M. E. E. Madden, R. J. Bodnar and J. D. Rimstidt, Nature, 431 (2004) 821.
2 D. T. Vaniman, D. L. Bish, S. J. Chipera, C. I. Fialips, J. William Carey and W. C. Feldman, Nature (London, United Kingdom), 431 (2004) 663.
3 J.-P. Bibring, Y. Langevin, F. Poulet, A. Gendrin, B. Gondet, M. Berthe, A. Soufflot, P. Drossart, M. Combes, G. Bellucci, V. Moroz, N. Mangold and B. Schmitt, Nature (London, United Kingdom), 428 (2004) 627.
4 B. M. Hynek, Nature (London, United Kingdom), 431 (2004) 156.
5 M. S. R. Swamy, T. P. Prasad and B. R. Sant, J. Thermal Anal., 16 (1979) 471.
6 M. S. R. Swamy, T. P. Prasad and B. R. Sant, J. Thermal Anal., 15 (1979) 307.
7 S. Bhattacharyya and S. N. Bhattacharyya, J. Chem. Eng. Data, 24 (1979) 93.
8 M. S. R. Swamy and T. P. Prasad, J. Thermal Anal., 19 (1980) 297.
9 M. S. R. Swamy and T. P. Prasad, J. Thermal Anal., 20 (1981) 107.
10 A. C. Banerjee and S. Sood, Therm. Anal., Proc. Int. Conf., 7th (1982) 769.
11 T. Buckby, S. Black, M. L. Coleman and M. E. Hodson, Mineralogical Magazine, 67 (2003) 263.
12 P. A. Williams, Oxide Zone Geochemistry, Ellis Horwood Ltd., Chichester, West Sussex, England 1990.
13 C. Drouet, D. Baron and A. Navrotsky, Am. Mineral., 88 (2003) 1949.
14 R. E. Stoffregen, C. N. Alpers and J. L. Jambor, Rev. Mineral. Geochem., 40 (2000) 453.
15 J. E. Dutrizac and J. L. Jambor, Rev. Mineral. Geochem., 40 (2000) 405.
16 G. Giuseppetti and C. Tadini, Neues Jahrbuch für Mineralogie, Monatshefte, (1980) 401.
17 K. Okada, J. Hirabayashi and J. Ossaka, Neues Jahrbuch für Mineralogie, Monatshefte, (1982) 634.
18 J. Ossaka, J. Hirabayashi, K. Okada, R. Kobayashi and T. Hayashi, Am. Mineral., 67 (1982) 114.
19 S. Aslanyan and R. Petrova, Geokhim., Mineral. Petrol., 3 (1975) 53.
20 A. I. Boldyrev, M. A. Klitchenko and G. A. Lyubarskaya, Obogashchenie Poleznykh Iskopaemykh, No. 3 (1968) 6.
21 Y. Cudennec, A. Riou, A. Bonnin and P. Caillet, Revue de Chimie Minérale, 17 (1980) 158.
22 S. V. Gevork'yan, Konstitutsiya i Svoistva Mineralov, 12 (1978) 54.
23 K. I. Petrov, V. G. Pervykh and N. K. Bol'shakova, Zh. Neorg. Khim., 11 (1966) 1392.
24 N. N. Poprukailo and T. B. Shkodina, Khim.-Metall. Inst., Karaganda, USSR, 1976, p. 12 pp.
25 N. T. Uklonskaya, Zapiski Uzbekistanskogo Otdeleniya Vsesoyuznogo Mineralogicheskogo Obshchestva, No. 25 (1972) 137.
26 K. Wada, Kanzei Chuo Bunsekishoho, 19 (1978) 133.
27 C. J. Serna, C. Parada Cortina and J. V. Garcia Ramos, Spectrochim. Acta, Part A: Molecular and Biomolecular Spectroscopy, 42A (1986) 729.
28 E. E. Coleyshaw, W. P. Griffith and R. J. Bowell, Spectrochim. Acta, Part A: Molecular and Biomolecular Spectroscopy, 50A (1994) 1909.
29 J. V. Garcia-Ramos and C. J. Serna, Revista de la Real Academia de Ciencias Exactas, Fisicas y Naturales de Madrid, 81 (1987) 397.
30 V. C. Farmer, Mineralogical Society Monograph 4: The Infrared Spectra of Minerals, 1974.
31 D. K. Arkhipenko and G. B. Bokii, Kristallografiya, 24 (1979) 100.

32 H. H. Adler and P. F. Kerr, Am. Mineral., 50 (1965) 132.
33 K. Sasaki, Can. Mineral., 35 (1997) 999.
34 K. Omori and P. F. Kerr, Geol. Soc. Am. Bull., 74 (1963) 709.
35 G. R. Hunt, Geophysics, 44 (1979) 1974.
36 D. K. Arkhipenko, E. T. Devyatkina and N. A. Pal'chik, Kristallokhimiya i Roentgenogr. Mineralov, L. (1987) 138.
37 K. Sasaki, O. Tanaike and H. Konno, Can. Mineral., 36 (1998) 1225.
38 C. Drouet and A. Navrotsky, Geochim. Cosmochim. Acta, 67 (2003) 2063.
39 J. M. Bouzaid, R. L. Frost, A. W. Musumeci and W. N. Martens, J. Therm. Anal. Cal., 86 (2006) 745.
40 R. L. Frost, J. Kristof, W. N. Martens, M. L. Weier and E. Horvath, J. Therm. Anal. Cal., 83 (2006) 675.
41 R. L. Frost, R.-A. Wills, J. T. Kloprogge and W. Martens, J. Therm. Anal. Cal., 84 (2006) 489.
42 R. L. Frost, R.-A. Wills, J. T. Kloprogge and W. N. Martens, J. Therm. Anal. Cal., 83 (2006) 213.
43 R. L. Frost, J. Kristof, M. L. Weier, W. N. Martens and E. Horvath, J. Therm. Anal. Cal., 79 (2005) 721.
44 R. L. Frost, M. L. Weier and W. Martens, J. Therm. Anal. Cal., 82 (2005) 115.
45 R. L. Frost and K. L. Erickson, J. Therm. Anal. Cal., 76 (2004) 217.
46 R. L. Frost, M. L. Weier and K. L. Erickson, J. Therm. Anal. Cal., 76 (2004) 1025.
47 R. L. Frost, Z. Ding and H. D. Ruan, J. Therm. Anal. Cal., 71 (2003) 783.
48 R. L. Frost and A. M. Vassallo, Clays Clay Miner., 44 (1996) 635.
49 R. L. Frost and A. M. Vassallo, Microchim. Acta, Suppl., 14 (1997) 789.
50 R. L. Frost and J. T. Kloprogge, Spectrochim. Acta, Part A, 55A (1999) 2195.
51 R. L. Frost and M. L. Weier, Thermochim. Acta, 406 (2003) 221.
52 J. Emsley, Chem. Soc. Rev., 9 (1980) 91.
53 H. Lutz, Struct. Bond. (Berlin, Germany), 82 (1995) 85.
54 W. Mikenda, J. Mol. Struct., 147 (1986) 1.
55 A. Novak, Struct. Bond. (Berlin), 18 (1974) 177.
56 E. Libowitsky, Monatsch. Chem., 130 (1999) 1047.
57 S. B. Hendricks, Am. Mineral., 22 (1937) 773.
58 S. Menchetti and C. Sabelli, Neues Jahrbuch für Mineralogie, Monatshefte, (1976) 406.
59 R. Wang, W. F. Bradley and H. Steinfink, Acta Cryst., 18 (1965) 249.
60 M. M. Shokarev, E. V. Margulis, F. I. Vershinina, L. I. Beisekeeva and L. A. Savchenko, Zh. Neorg. Khim., 17 (1972) 2474.
61 J. Kubisz, Miner. Pol., 3 (1972) 23.

Received: October 19, 2006
Accepted: February 28, 2007
OnlineFirst: October 14, 2007

DOI: 10.1007/s10973-006-7979-2